

ESI

Highly Selective Luminescent Sensor for CCl_4 Vapor and Pollutional Anions/Cations based on a Multi-responsive MOF

Fei-Yan Yi,* Shi-Cheng Wang, Minli Gu, Jia-Qi Zheng, and Lei Han*

Table S1. Selected bond lengths and bond angles for NBU-18.

Cd(1)-O(5)#1	2.227(4)	Cd(2)-O(6)#2	2.171(5)
Cd(1)-O(5)#2	2.227(4)	Cd(2)-N(1)	2.239(5)
Cd(1)-O(8)#3	2.300(5)	Cd(2)-O(10)#5	2.260(5)
Cd(1)-O(8)	2.300(5)	Cd(2)-O(8)	2.342(5)
Cd(1)-O(9)#4	2.303(5)	Cd(2)-O(7)	2.373(5)
Cd(1)-O(9)#5	2.303(5)	Cd(2)-O(9)#5	2.567(5)
O(1)-C(2)#8	1.413(8)	O(9)-Cd(1)#4	2.303(5)
O(5)-Cd(1)#9	2.227(4)	O(9)-Cd(2)#6	2.567(5)
O(6)-Cd(2)#9	2.171(5)	O(10)-Cd(2)#6	2.260(5)
O(5)#1-Cd(1)-O(5)#2	180.000(1)	O(8)-Cd(2)-O(9)#5	75.37(17)
O(5)#1-Cd(1)-O(8)#3	88.53(19)	O(8)-Cd(2)-O(7)	54.26(17)
O(5)#1-Cd(1)-O(8)	91.47(19)	O(8)-Cd(1)-O(9)#4	98.5(2)
O(5)#1-Cd(1)-O(9)#4	89.59(17)	O(8)-Cd(1)-O(9)#5	81.5(2)
O(5)#1-Cd(1)-O(9)#5	90.41(17)	O(8)#3-Cd(1)-O(8)	180.000(1)
O(5)#2-Cd(1)-O(8)#3	91.47(19)	O(8)#3-Cd(1)-O(9)#4	81.5(2)
O(5)#2-Cd(1)-O(8)	88.53(19)	O(8)#3-Cd(1)-O(9)#5	98.5(2)
O(5)#2-Cd(1)-O(9)#4	90.41(17)	O(9)#4-Cd(1)-O(9)#5	180.000(1)
O(5)#2-Cd(1)-O(9)#5	89.59(17)	O(10)#5-Cd(2)-O(8)	98.0(2)
O(6)#2-Cd(2)-N(1)	94.3(2)	O(10)#5-Cd(2)-O(7)	102.6(2)
O(6)#2-Cd(2)-O(10)#5	132.0(2)	O(10)#5-Cd(2)-O(9)#5	53.76(18)
O(6)#2-Cd(2)-O(8)	94.3(2)	N(1)-Cd(2)-O(10)#5	103.9(2)
O(6)#2-Cd(2)-O(7)	121.8(2)	N(1)-Cd(2)-O(8)	141.3(2)
O(6)#2-Cd(2)-O(9)#5	85.57(19)	N(1)-Cd(2)-O(7)	89.7(2)
O(7)-Cd(2)-O(9)#5	121.73(17)	N(1)-Cd(2)-O(9)#5	142.9(2)

Symmetry transformations used to generate equivalent atoms:

#1 -x+3/2, -y+3/2, -z+2; #2 x, y, z-1; #3 -x+3/2, -y+3/2, -z+1; #4 -x+2, y, -z+3/2; #5 x-1/2, -y+3/2, z-1/2; #6 x+1/2, -y+3/2, z+1/2; #7 -x+3/2, -y+1/2, -z+1; #8 -x+2, y, -z+5/2; #9 x, y, z+1.

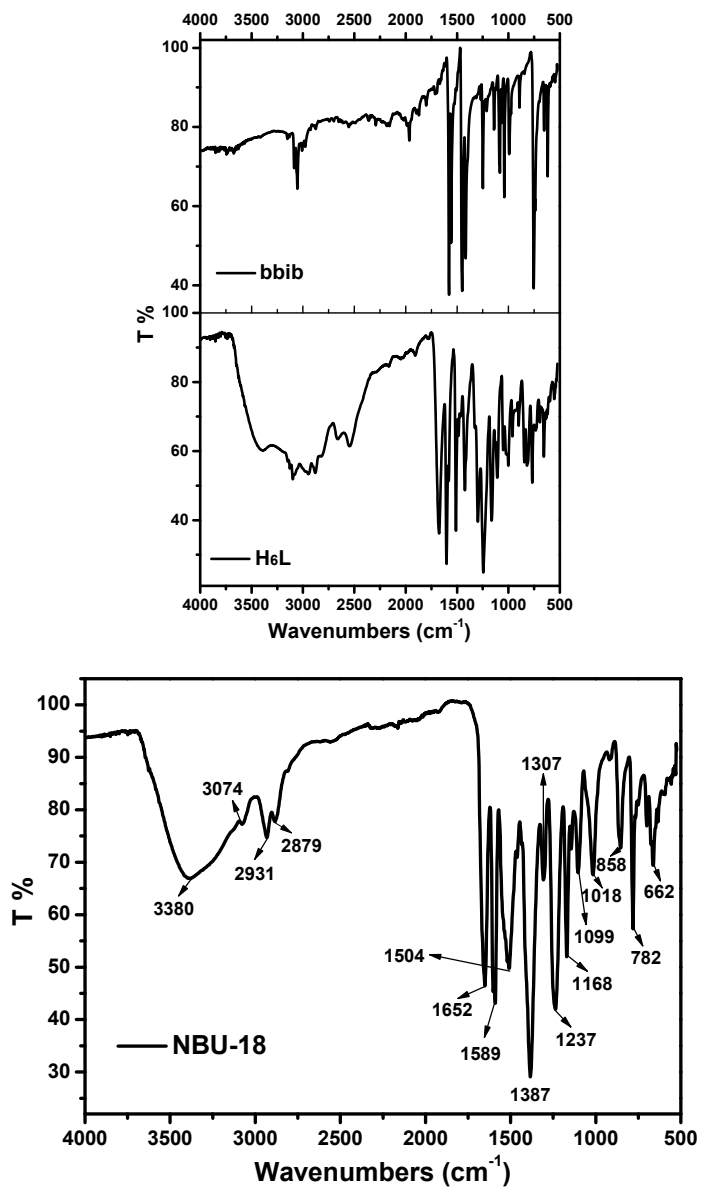
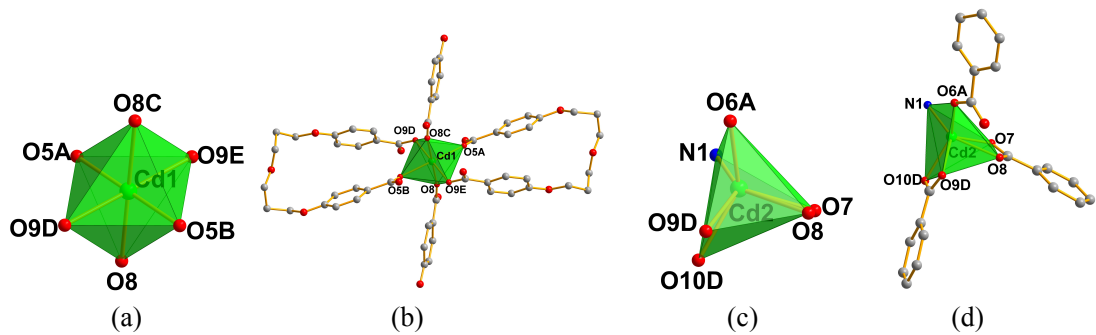


Fig. S1 FT-IR spectra of free H_6L , bbit, and MOF NBU-18.



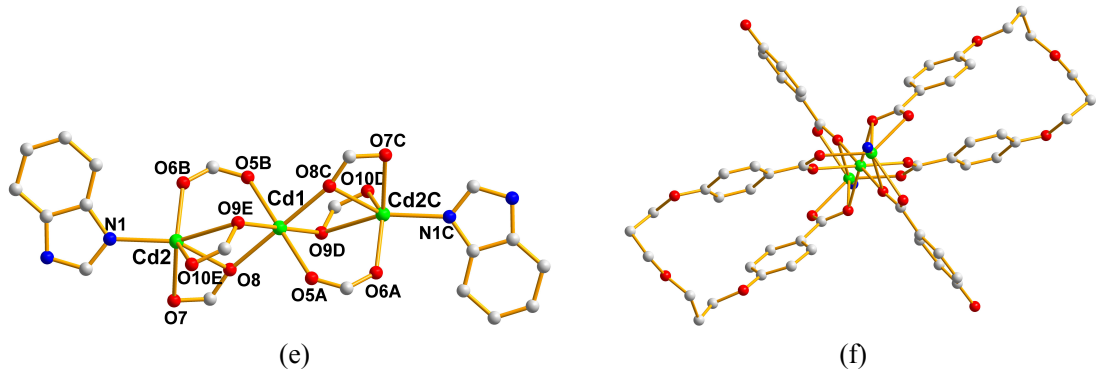


Fig. S2 The coordinated mode of metal center Cd1 (a, b), Cd2 (c, d), and Cd_3^{II} SBU (e, f).

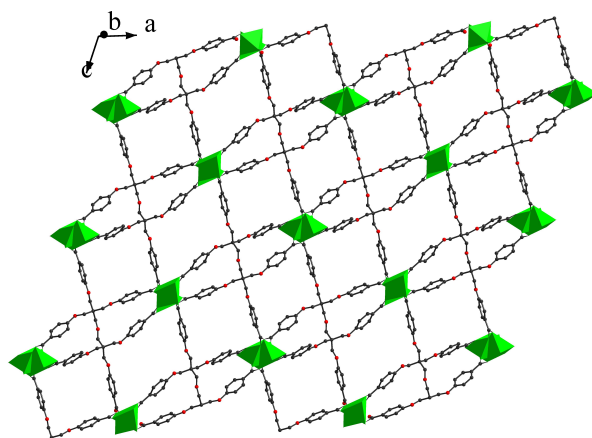


Fig. S3 The 2D Cd-L layer along *b*-axis. The CdO_xN_y ($x = 5$ or 6, $y = 1$ or 0) polyhedra were drawn in green. C and O atoms were shown in black and red balls, respectively.

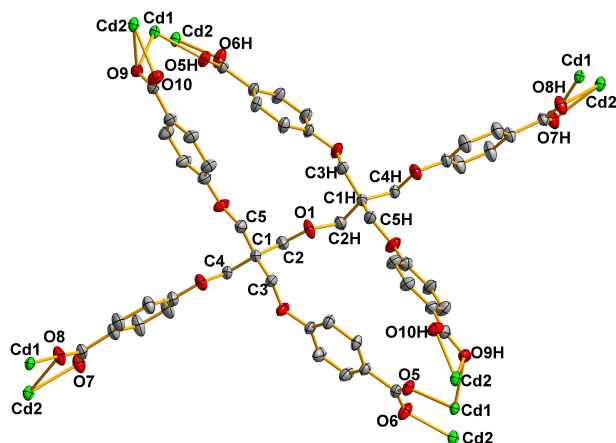
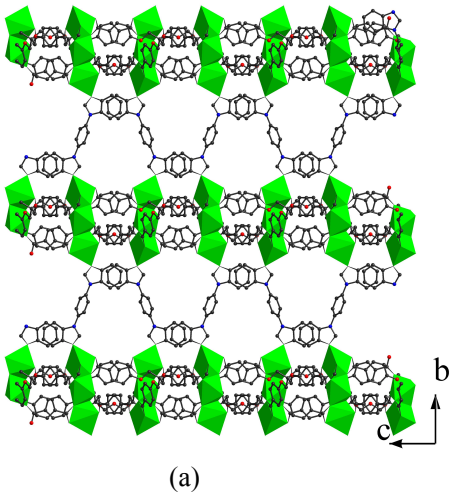
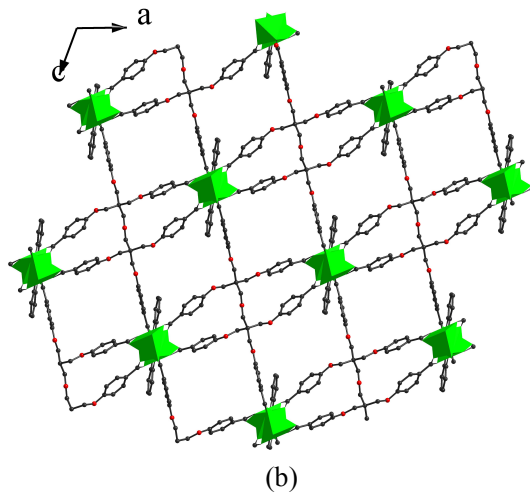


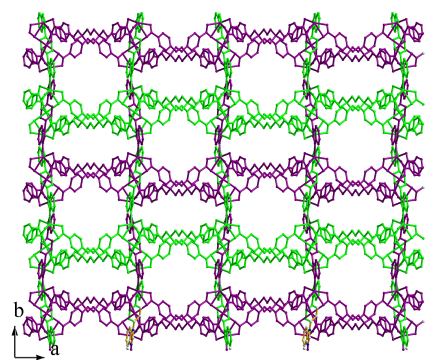
Fig. S4 The coordinated environment of L^{6-} .



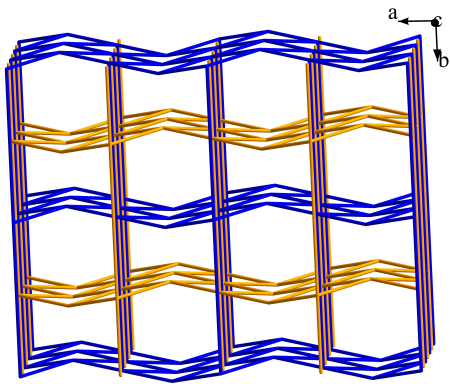
(a)



(b)

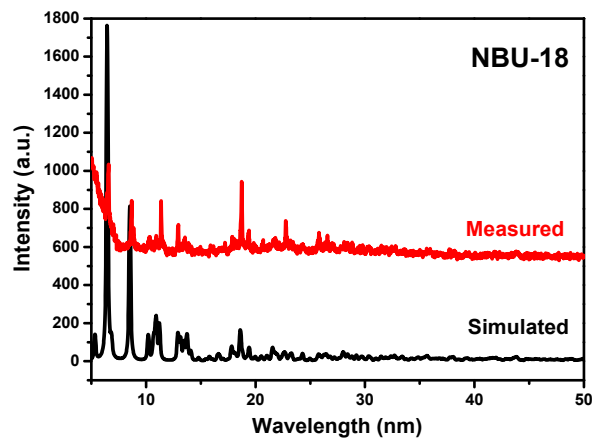


(c)

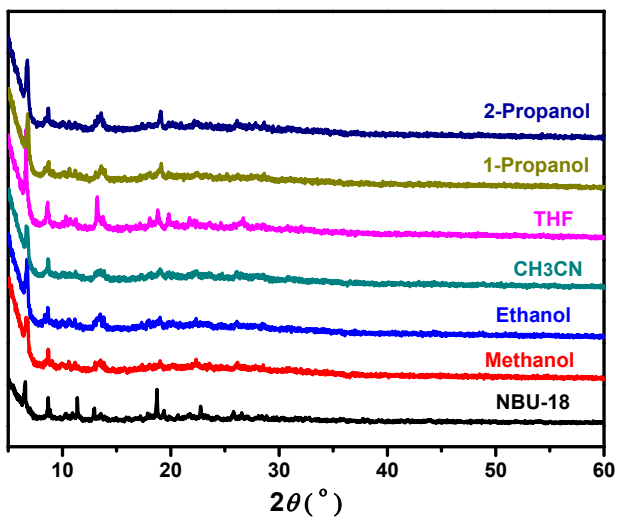


(d)

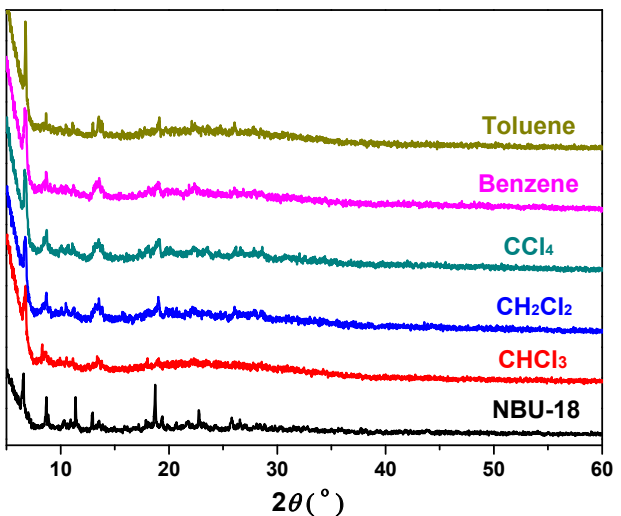
Fig. S5 View the 3D one-fold net along *a*-axis (a), and *b*-axis (b). The 2-fold interpenetrated 3D net (c) and the corresponding simplified 2-nodal *fsc* net (d) along *c*-axis.



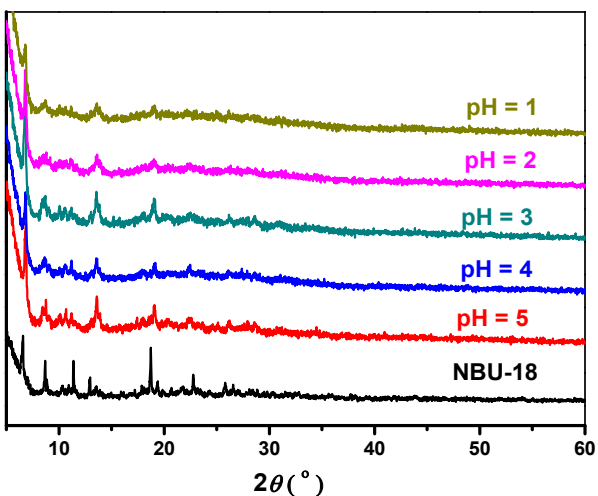
(a)



(b)



(c)



(d)

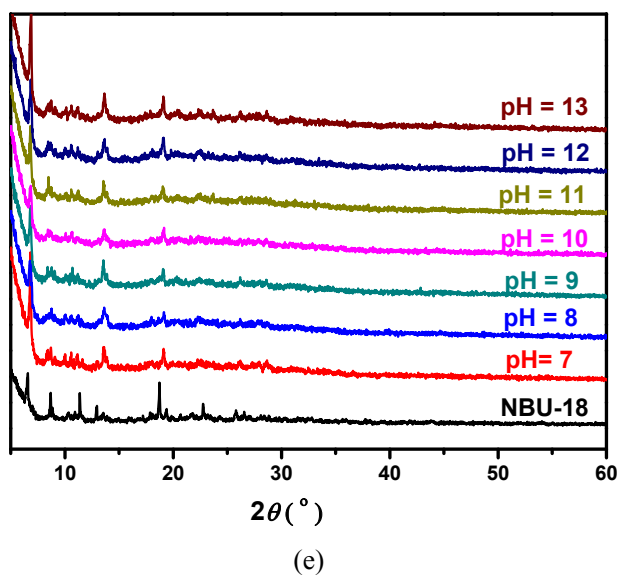


Fig. S6 (a) The PXRD patterns of as-synthesized sample NBU-18 (red, measured) and the calculated pattern (black, simulated) from its crystal structure. (b and c) The PXRD patterns of NBU-18 samples after immersed into various solvents for 24 h. (d and e) The PXRD patterns of NBU-18 samples after immersed into different pH aqueous solutions for 12 h.

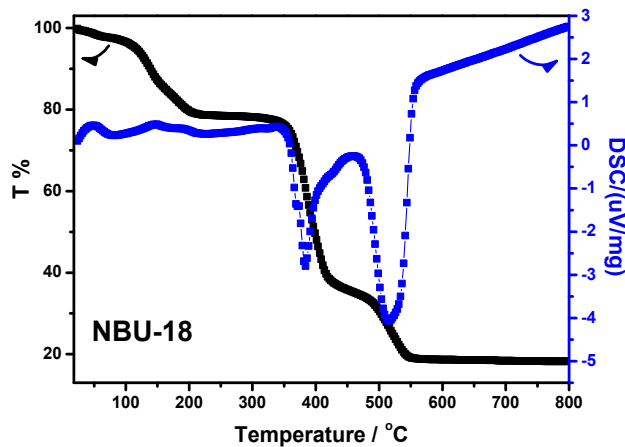


Fig. S7 TG-DSC curves of **NBU-18** under N_2 atmosphere at a heating rate of $10\text{ }^{\circ}\text{C}/\text{min}$.

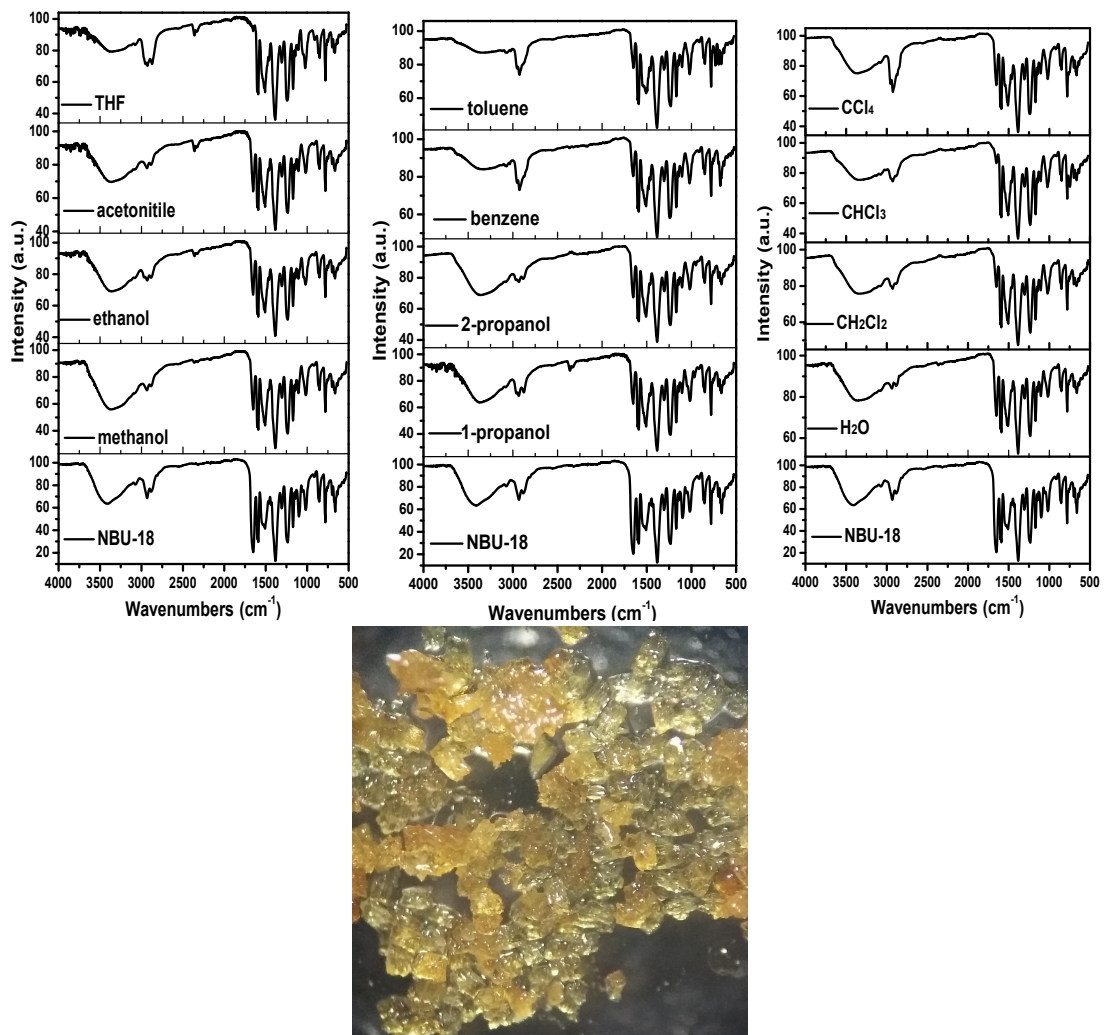


Fig. S8. FTIR spectra of MOF NBU-18 samples after treatment in various solvents for 24 hours and image of NBU-18 crystals after treatment in various solvents.

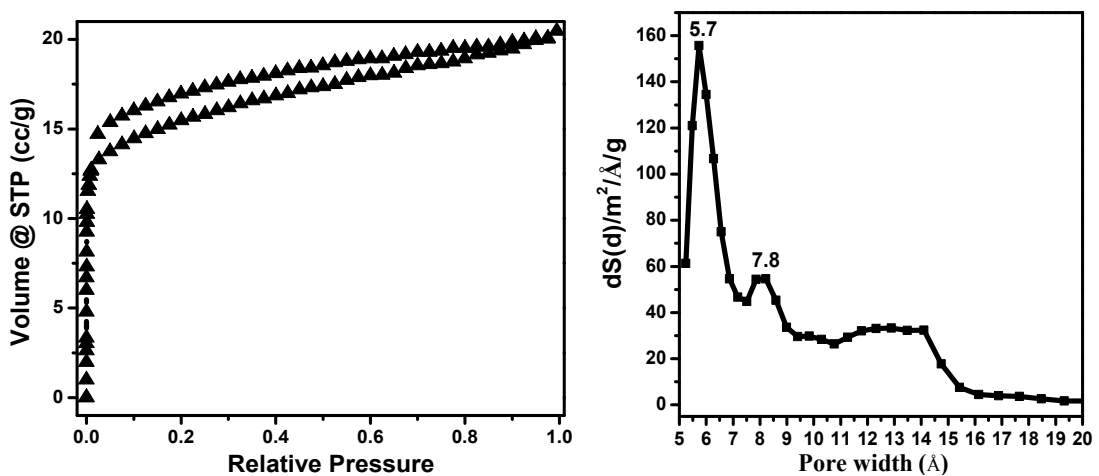


Fig. S9 Gas adsorption-desorption isotherm and pore size distribution of NBU-18 for N₂ at 77 K. Considering the structure features of NBU-18 compound with a high-solvent-accessible volume of 4085.8 Å³ (42.3%) of the crystal unit cell volume (9665.2 Å³) based on PLATON calculation and three sets of channels with 20.8 × 14.7 Å² along *c*-axis, 10.4 × 8.5 Å² along *a*-axis, and 9.0 × 8.8

\AA^2 along *b*-axis (including van der Waals radius), its gas adsorption isotherm for N_2 at 77 K was performed on ASAP 2050 V1.01 E and Autosorb MP-1 apparatuses at 1 atm. Prior to the measurement, the as-synthesized sample of NBU-18 was immersed in methanol for three days, the methanol was refreshed three times during the exchange. The resulting methanol-exchanged sample of NBU-18 was transferred into dichloromethane solvent for 12 h. Similarly, fresh dichloromethane was also exchanged for three times. The resulting exchanged sample was then evacuated (10^{-3} Torr) successively at room temperature and 80 °C. As shown in Fig. S9, the NBU-18 exhibits a single step type I sorption behavior with a relatively small N_2 gas sorption amount ($54.3 \text{ cm}^3 \text{ g}^{-1}$). Its pore size distribution (5.7 \AA and 7.8 \AA) matches well with the crystal structure model.

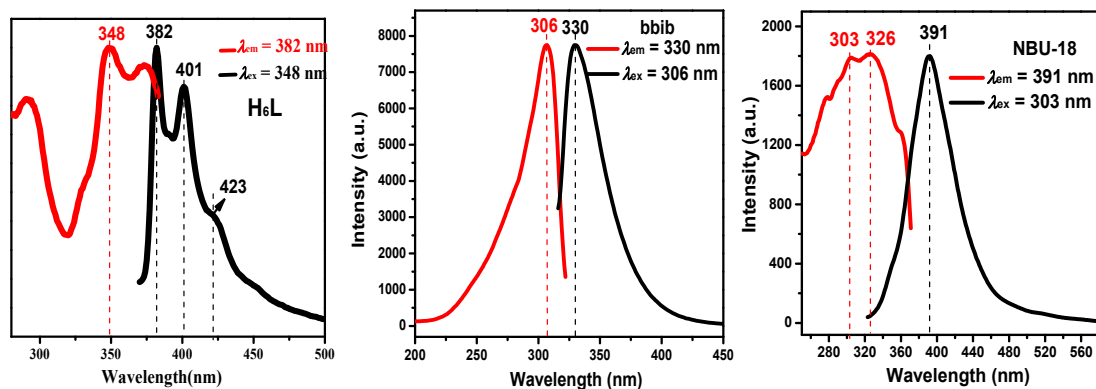


Fig. S10. The solid-state emission and excitation spectra of NBU-18 as well as the emission spectra of free H₆L and bbib ligands.

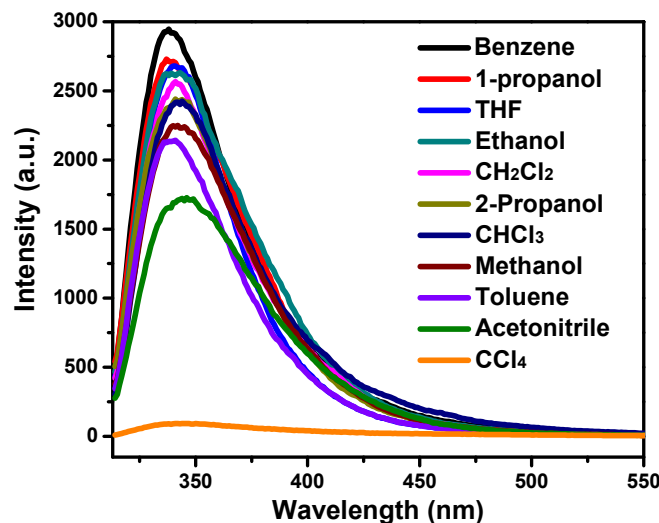


Fig. S11 Emission spectra of NBU-18 in various organic solvents at room temperature ($\lambda_{\text{ex}} = 291 \text{ nm}$)

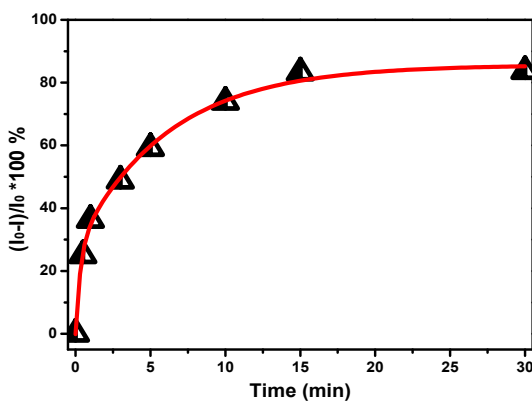


Fig. S12. The relationship between fluorescence quench percentage of PL intensity for NBU-18 and exposing time for CCl_4 vapor, in which I_0 and I = the fluorescence intensity of the emulsion in the absence and presence of CCl_4 vapor, respectively.

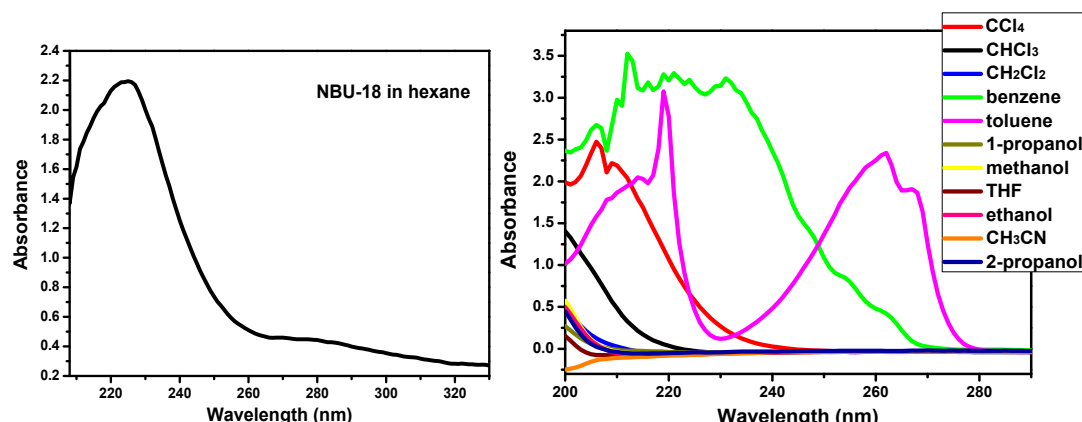


Fig. S13. The UV-vis spectra of various organic solvents and NBU-18 in hexane at room temperature.

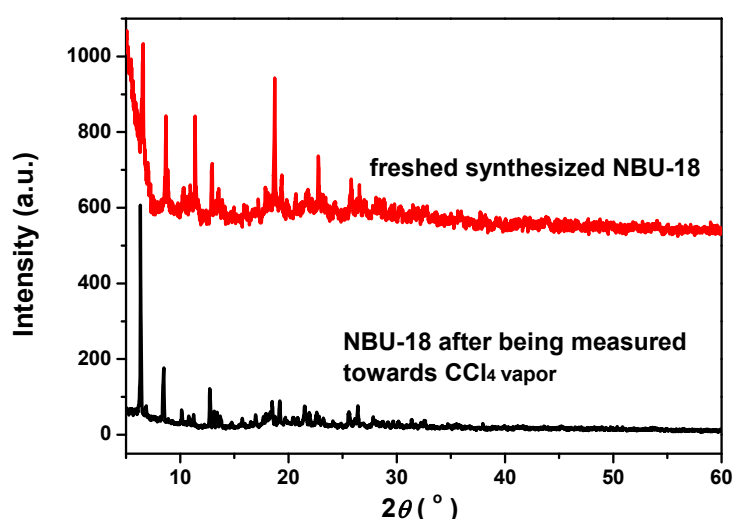


Fig. S14 The PXRD pattern of NBU-18 after being measured toward CCl_4 vapor for 12 h.

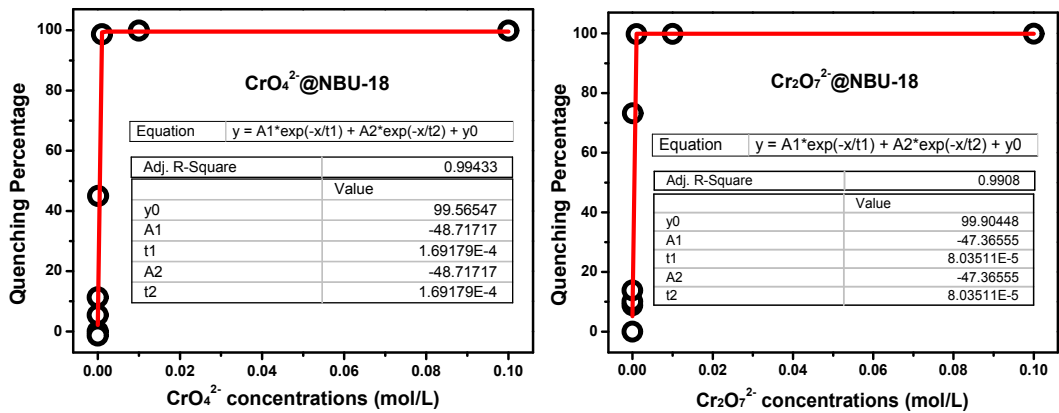


Fig. S15. The relationship between fluorescence quench percentage of PL intensities fro NBU-18 and the concentration of Cr₂O₇²⁻ and CrO₄²⁻, respectively.

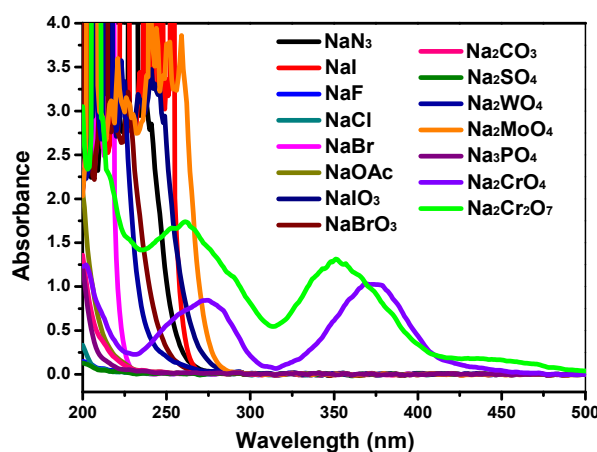


Fig. S16. The UV-vis spectra of the aqueous solutions with different anions at room temperature.

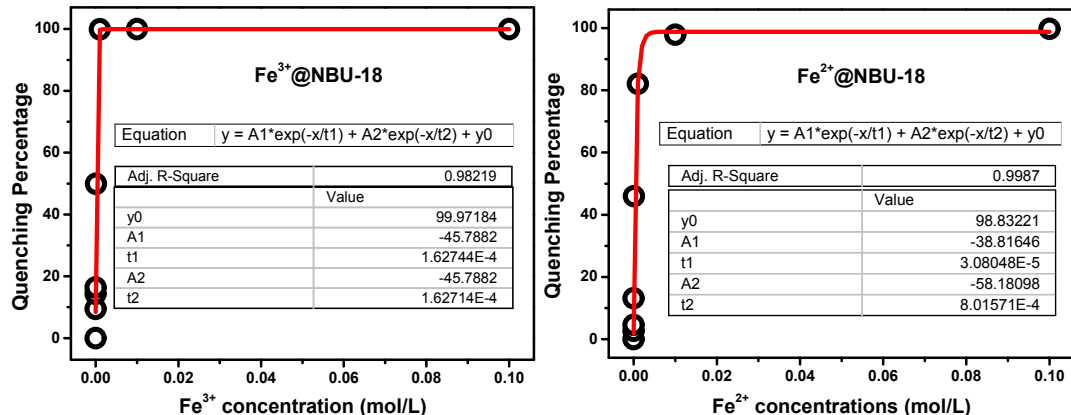


Fig. S17 The relationship between fluorescence quench percentage of PL intensities fro NBU-18 and the concentration of Fe²⁺ and Fe³⁺, respectively.

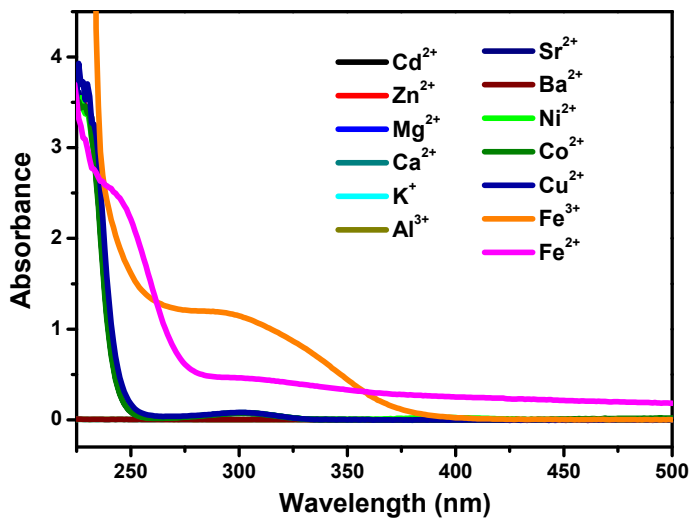
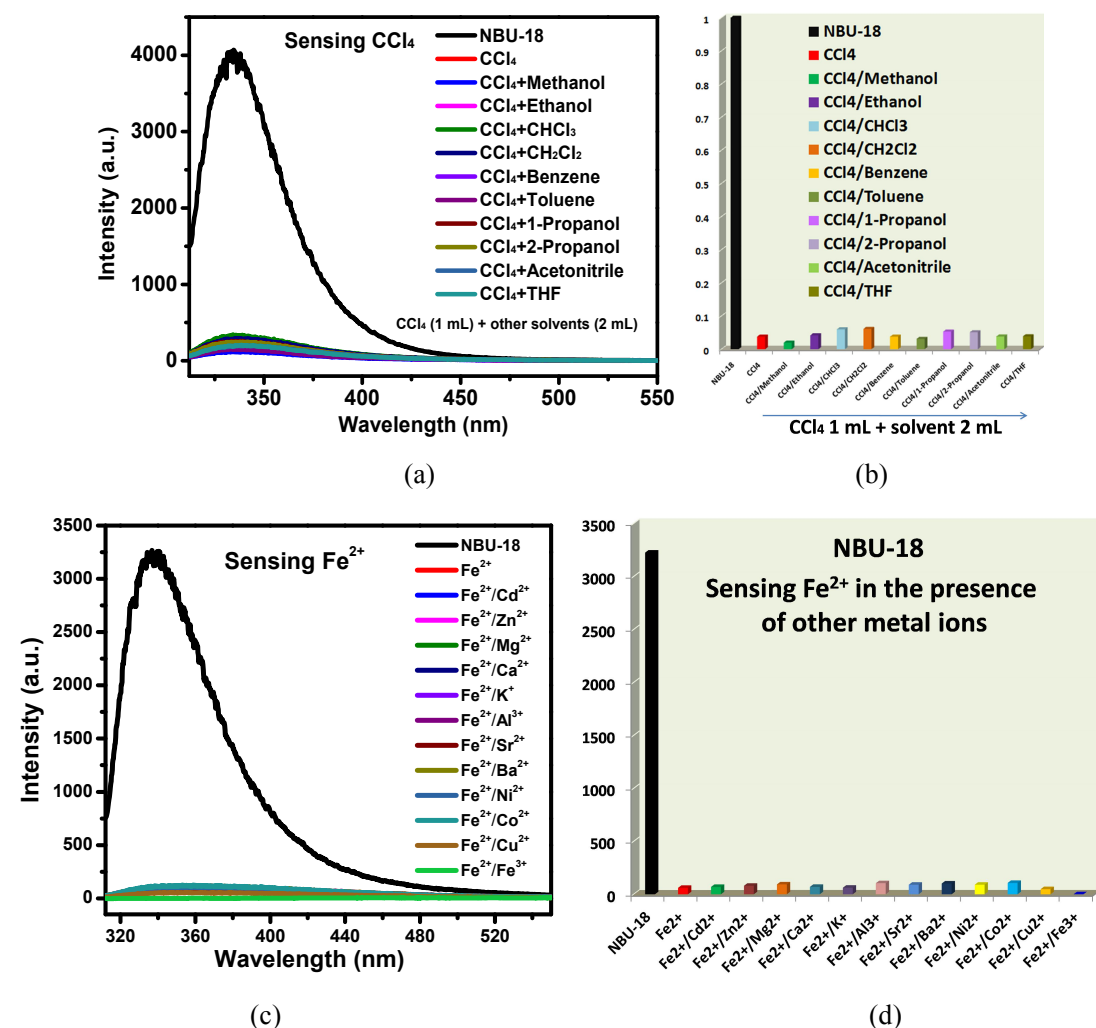


Fig. S18 The UV-vis spectra of the aqueous solutions with different cations at room temperature.



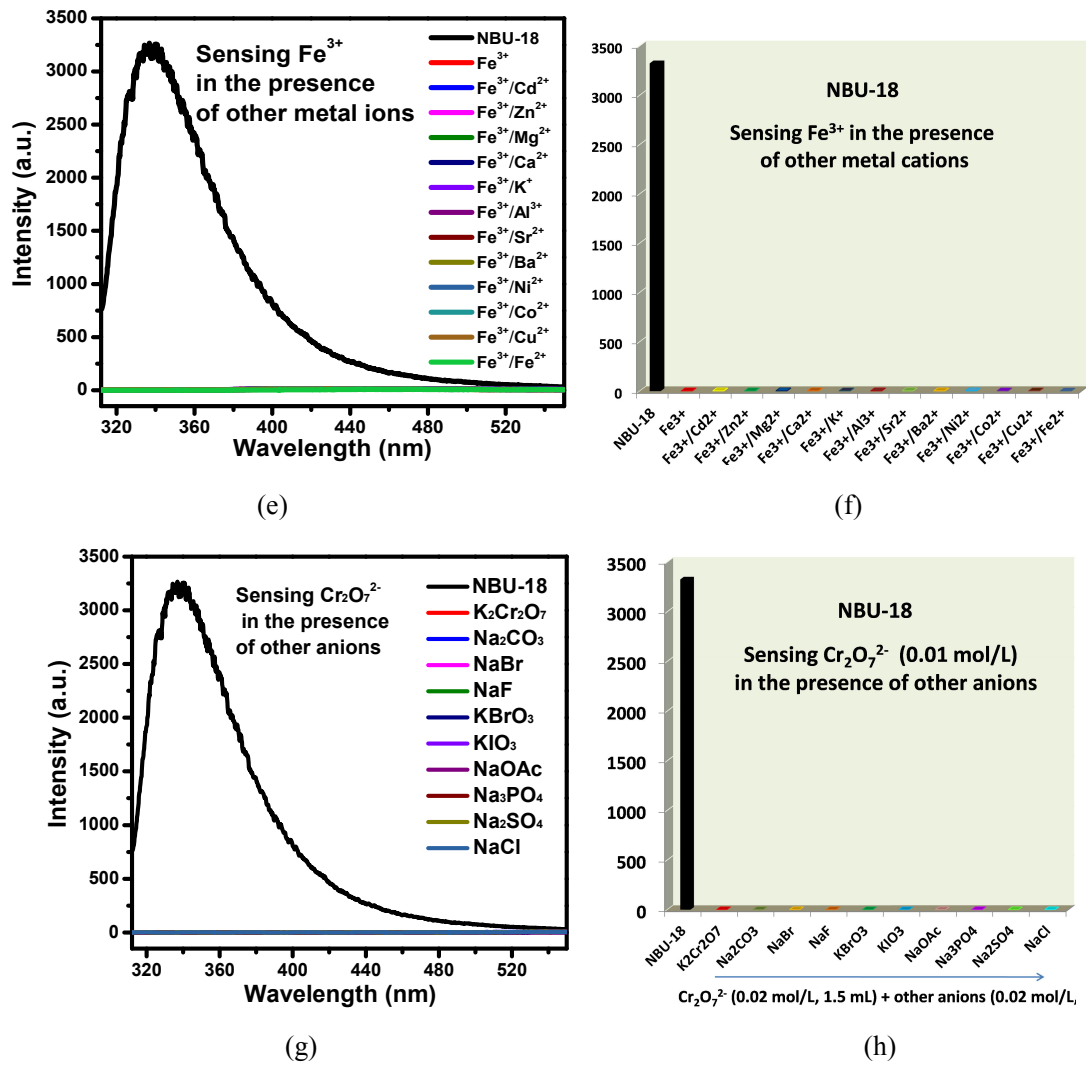


Fig. S19 (a and b) Luminescence spectra and intensities and of NBU-18 in mixed solvents of CCl_4 (1 mL) and other organic solvents (2 mL) under the excitation of 291 nm. (c and d) The luminescence spectra and its intensity of the aqueous solutions of NBU-18 in the presence of Fe^{2+} (0.01 mol/L) and other cations (0.01 mol/L). (e and f) The luminescence spectra and its intensity of the aqueous solutions of NBU-18 in the presence of Fe^{3+} (0.01 mol/L) and other cations (0.01 mol/L). (g and h) The luminescence spectra and its intensity of the aqueous solutions of $\text{Cr}_2\text{O}_7^{2-}$ @ NBU-18 (0.01 mol/L) in the presence of various anions (0.01 mol/L).

The anti-interference sensing experiments were prepared as follows and were carried out.

- NBU-18 sample of 5 mg was added into the CCl_4 solvent (1 mL), further introducing various other solvents of 2 mL, containing methanol (CH_3OH), ethanol (EtOH), trichloromethane (CHCl_3), dichloromethane (CH_2Cl_2), tetrachloromethane (CCl_4), benzene, toluene, 1-propanol, 2-propanol, acetonitrile (CH_3CN) and tetrahydrofuran (THF), respectively.
- NBU-18 sample of 5 mg was added into the aqueous solution of Fe^{2+} (0.02 mol/L, 1.5 mL), then adding various aqueous solutions with other metal cations (0.02 mol/L, 1.5 mL) containing K^+ , Mg^{2+} , Ca^{2+} , Sr^{2+} , Ba^{2+} , Al^{3+} , Cd^{2+} , Zn^{2+} , Fe^{2+} , Fe^{3+} , Co^{2+} , Ni^{2+} , Cu^{2+} , to keep the concentration of Fe^{2+} at 0.01 mol/L in aqueous solution when other metal ions were introduced into the NBU-18 system. For Fe^{3+} , similar preparation was carried out except for Fe^{3+} (0.02 mol/L, 1.5 mL) instead of Fe^{2+} aqueous solution.

(c) NBU-18 sample of 5 mg was added into the aqueous solution of $\text{Cr}_2\text{O}_7^{2-}$ (0.02 mol/L, 1.5 mL), then adding various aqueous solutions with other anions (0.02 mol/L, 1.5 mL) containing CO_3^{2-} , Br^- , F^- , BrO_3^- , IO_3^- , CH_3COO^- (OAc^-), PO_4^{3-} , SO_4^{2-} , Cl^- , $\text{Cr}_2\text{O}_7^{2-}$, to keep the concentration of $\text{Cr}_2\text{O}_7^{2-}$ at 0.01 mol/L in aqueous solution when other anions were introduced into the NBU-18 system.

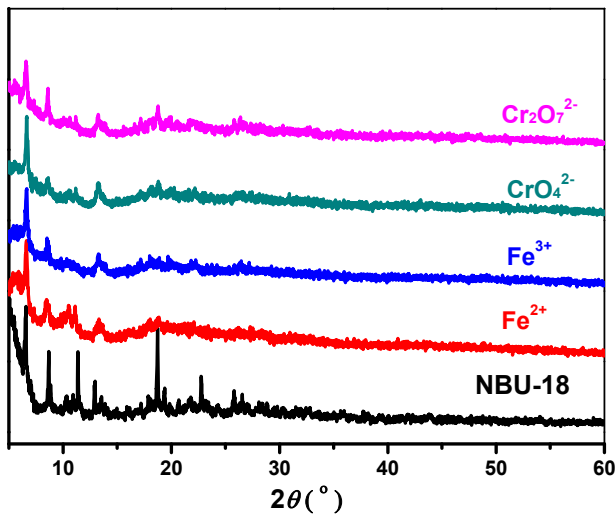


Fig. S20 The PXRD pattern of freshly synthesized NBU-18 and the ones after being measured toward $\text{Fe}^{2+}/\text{Fe}^{3+}$, $\text{CrO}_4^{2-}/\text{Cr}_2\text{O}_7^{2-}$ ions.

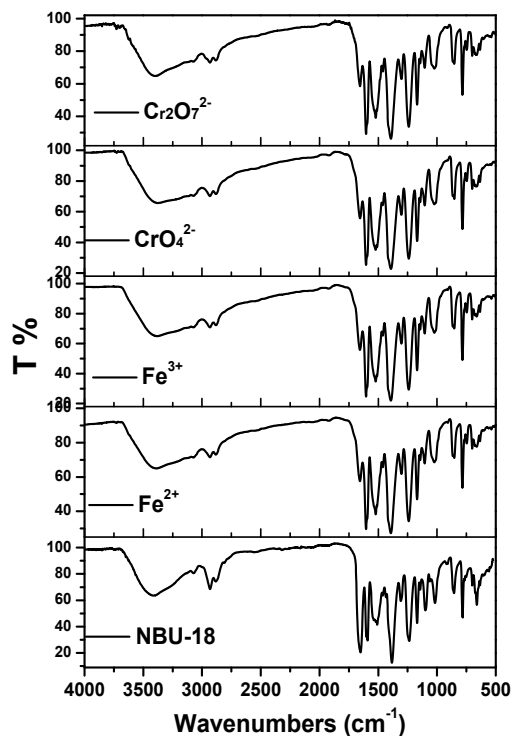


Fig. S21 The FT-IR spectra of freshly synthesized NBU-18 and the ones after being measured toward $\text{Fe}^{2+}/\text{Fe}^{3+}$, $\text{CrO}_4^{2-}/\text{Cr}_2\text{O}_7^{2-}$ ions.